

Branching mechanism of intergranular crack propagation in three dimensions

M. Itakura and H. Kaburaki

*Center for Promotion of Computational Science and Engineering,
Japan Atomic Energy Research Institute, Taito-ku, Higashiueno 6-9-3, Tokyo 110-0015, Japan*

C. Arakawa

Interfaculty Initiative in Information Studies, University of Tokyo, 7-3-1 Hongo, Bunkyo-ku, Tokyo 113, Japan

(Dated: November 17, 2018)

We investigate the process of slow intergranular crack propagation by the finite element method model and show that branching is induced by partial arresting of a crack front owing to the geometrical randomness of grain boundaries. A possible scenario for the branching instability of crack propagation in a disordered continuous medium is also discussed.

PACS numbers: 62.20.Mk, 81.40.Np, 46.50.+a

The morphology of cracks has been the subject of intensive studies in recent years. Experimental observations of the universal roughness exponent $\eta \sim 0.8$ of the fracture surface [1, 2] have been stimulating theoretical and numerical studies of relevant models. Another interesting subject is the branching behavior of fast-propagating cracks: There seems to be a dynamic branching instability that is common in various kinds of amorphous materials [3], and this branching instability has been numerically reproduced [4, 5]. In the brittle fracture of gels, a different kind of branching has been observed [6].

Branching is also observed in slowly propagating cracks such as intergranular stress corrosion cracking (IGSCC), which occurs when a polycrystalline metal or alloy is subjected to both tensile stress and a corrosive environment (See Fig. 1), such as nuclear reactor coolant (irradiated water). The corrosive agent selectively corrodes the grain boundary (GB) near the crack tip, which is under tensile stress, and the crack propagates along the GBs exhibiting typical branching patterns. Empirical relations between the mode-I stress intensity factor K_I at the crack tip and crack propagation velocity v is used to assess the safety of structural materials, and they usually take power-law form $v = C(K_I - K_{Ic})^a$, where C and a are parameters that depend both on material and environment, and K_{Ic} is a critical value of K_I at which the crack begins to propagate. The typical velocity of crack propagation of IGSCC under an industrial environment is of the order 0.1 to 1 mm per year.

Naively, the branching of intergranular cracking may seem obvious because there are numerous GB triple junctions where a crack front has a chance to branch, but in reality, it is not so simple: If a branch occurred at a triple junction, the stress concentrates on the longer branch and thus enhances its propagation, screening the stress of shorter branch, eventually suppressing its propagation before it grows to a length compatible with the GB length. In the present paper, we model the intergranular crack propagation process and carry out numerical simulations, and show that the branching occurs even when the explicit branching at GB triple junctions is forbidden.

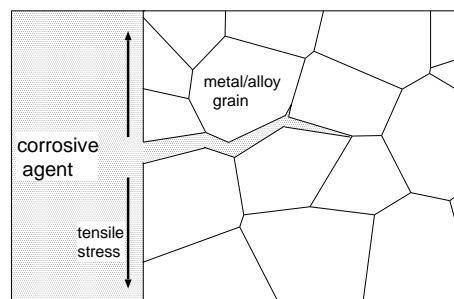


FIG. 1: Schematic depiction of intergranular stress corrosion cracking. A corrosive agent diffuses through the opened crack and corrodes grain boundaries under tensile stress.

At the first stage of the simulation, polycrystalline GBs are prepared using random Voronoi tessellation [7] of a cube of dimensionless size $1.0 \times 1.0 \times 1.0$, and a crack is assumed to propagate through these GBs. In this paper, 12 000 grains are used. Tensile stress along the y axis (see Fig. 2) is applied as constant loads on the $y = 0$ and $y = 1$ plane of the cube, and local stress distribution (by which the crack is driven) is calculated using a simplified finite-element-method (FEM) model. The FEM nodes are placed at vertices of grains, centers of GB surfaces, and centers of grains. Each grain is decomposed into tetrahedral FEM elements, which contain two vertex nodes, one surface center node, and one grain center node (Fig. 3(a)). To glue the grains together, a very thin FEM element is placed at each GB, which is made up of six-node triangular elements (Fig. 3(b)). The thickness of this gluing element is set to 10^{-4} . When a GB fails, the elastic constants of the corresponding gluing element are set to zero. To enhance the stress concentration at the crack tip, the initial crack is prepared by separating all the GBs between two grains whose grain centers are above and below a plane $y = 0.5$ and lie in a region $z < 0.2$. The crack then proceeds in the z direction.

The most crucial and difficult part of this kind of modeling studies is a determination of the crack propagation rule. In this paper, a certain GB is selected based

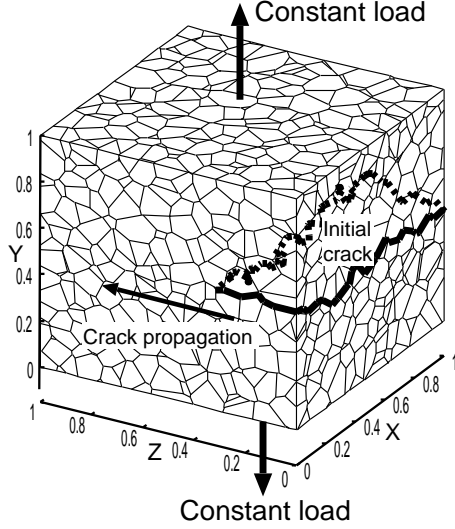


FIG. 2: Geometry of a simulation cell. An initial crack is placed at a region $y \sim 0.5$, $z < 0.2$ and constant load is imposed on the upper ($y = 1$) and lower ($y = 0$) surface of the cube.

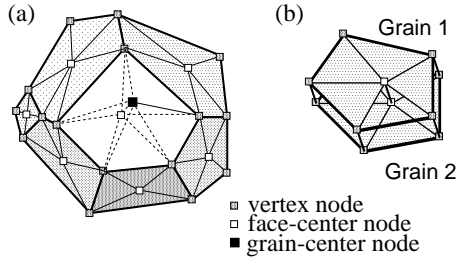


FIG. 3: Construction of FEM elements. (a) Nodes are placed at vertex, face center, and body center of each grain. (b) Each grain is glued together by thin triangular elements.

on the stress distribution, and is separated completely. Therefore the GBs fail one at a time, which is similar to the rule employed in the so-called network models, such as random fuse models [8] and random spring models [9]. Although the validity of this rule for the simulation of intergranular cracking is quite unclear because the nearby stress distribution may change significantly while the crack front proceeds through the selected GB and may initiate another GB failure, there are two reasons why we employ this rule. Firstly, to track the continuous propagation of the crack front along a GB requires very fine FEM meshing around the crack tip, or alternatively, the FEM mesh must be reorganized around the crack tip each time the crack proceeds by a small amount. Both methods require extensive computational power and a fairly complex simulation code, and the number of grains will be severely restricted. Secondly, it is plausible to assume that the crack front is arrested at the triple junctions of GBs for a long time; thus the propagation process may be treated as a series of discrete events of GB failure.

The rule to determine which GB to separate is that we

choose a GB on which the strongest tensile stress normal to its surface is imposed. Considering that the stress diverges near the crack tip as $K_I r^{-1/2}$ in the linear elastic theory, where r is a distance to the crack tip and K_I is a mode-I stress intensity factor, we choose among the GBs that are adjacent to the crack tip. In the present model, the crack tip is defined as a set of GB triple junctions that is shared by one fractured and two unfractured GBs. This restriction forbids explicit branching at triple junctions, as well as isolated crack initiation in the unfractured interior, and distinguishes the present model from the network models that are mainly used to study crack morphology. After the selected GB fails, the elastic matrix is updated and the fracture process is repeated.

Local stress is calculated by standard linear elastic theory [10]. Since only the linear theory is used in the present paper, one can arbitrarily scale the stress and strain. We set Young's modulus E to unity and assume the elastic properties to be isotropic; therefore the only elastic parameter to be considered is Poisson's ratio ν , and simulations are carried out for several values of ν . To evaluate the tensile stress acting on a GB, a normal component of a difference of displacements between two nodes that lie on both sides of the gluing element is calculated at each vertex of a GB. Here we only investigate vertices on the crack tip, where maximum of tensile stress occurs. The FEM mesh we use is very coarse compared to engineering studies, in which progressively finer mesh is used around the crack tip. However, the main concern in the engineering studies is to evaluate precisely a stress intensity factor at the crack tip and to determine whether it is greater than the critical value above which the crack propagates catastrophically. Therefore, in these studies, the initial crack is usually assumed to be a semicircular microcrack and the propagation process is not studied.

There have been several numerical studies of intergranular crack propagation in which some simplifying approximations are used, such as redistributing the stress of a failed surface equally to the neighbor surfaces [11]. The present paper simulates and evaluates intergranular cracking process with full geometrical modeling of three-dimensional grain boundaries and evaluates an approximate local stress field (if crude) by which crack is driven. A system of linear equations has been solved using the BiCG-stab (bi-conjugate gradient stabilized) iterative solver. The dimension of the vector was about 1 500 000, and the number of nonzero elements of the symmetric elastic matrix was about $28\,000\,000 \times 2$ in the case of 12 000 grains. Most of the CPU time of the simulation was spent in the solver routine, which has been vectorized and run on a NEC SX-6 vector processor. The overall CPU time needed to carry out 1 500 steps of GB fracture was about 6 h.

Figure 4 shows fracture surface projected onto the $X-Z$ plane, obtained from the simulation of the $\nu = 0.25$ case: the black area shows the fracture surface, and the light gray areas show the branched fracture surfaces. In this case, more than 20 percent of the fracture surface

area (projected onto the $X - Z$ plane) is covered by the branched surface, even though explicit branching at GB triple junctions is forbidden. Figure 5 shows convergence of the ratio of the branch surface plotted against the projected fracture surface area for the three typical cases of $\nu = 0.0$ (spongy), $\nu = 0.25$ (a typical value of metals), and $\nu = 0.49$ (rubbery). It can be seen that in each case the ratio converges to a value 0.2–0.3, and the branching behavior does not vary drastically, even in the extreme cases of $\nu = 0.0$ and $\nu = 0.49$.

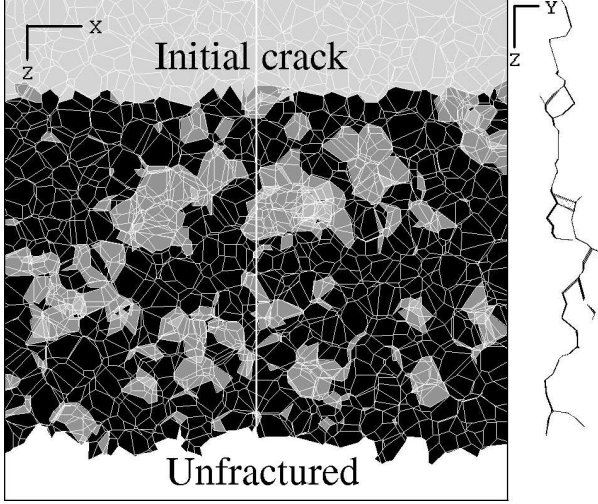


FIG. 4: Fractured surface observed in the simulation of $\nu = 0.2$ case, projected onto the $X - Z$ plane. The black and gray areas show the fracture surface and branch fracture surface, respectively. The cross section of the fracture surface in the center (bold white line) is shown on the right side.

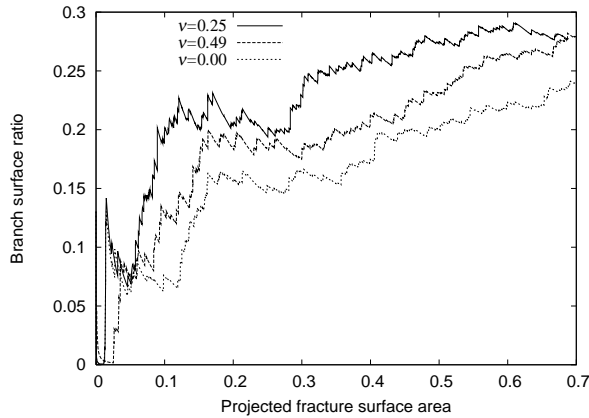


FIG. 5: Ratios of branch surface area plotted against the projected fracture surface area for several values of Poisson's ratio ν .

Figure 6 schematically depicts the typical branching mechanism observed in the simulation: (a) The crack front is arrested at the sloped surface $S0$, where mode-I stress is reduced by a factor of $\cos\theta$ where θ is the inclination angle of $S0$ out of the $X - Z$ plane. (b) The crack

initiates at the point v and propagates along the much horizontal surface $S1$, and intersects the fracture surface at the segment $L0$. After this kind of branch is formed, the branched crack front circumvents the arresting GB and continues propagation, and eventually merges again to resume intact crack front line and leaves a branch behind that consists of several GBs. Although the branch length is only of an order of several GBs, so frequent a branching, as observed in this simulation, will significantly affect the crack propagation velocity if we would construct a time-driven crack propagation rule and simulate it. As for the long-length scale properties of the fracture surface, an estimate of roughness exponent is of interest, but the obtained fracture surface, which consists of about 1 500 GBs, is not large enough to observe such quantities.

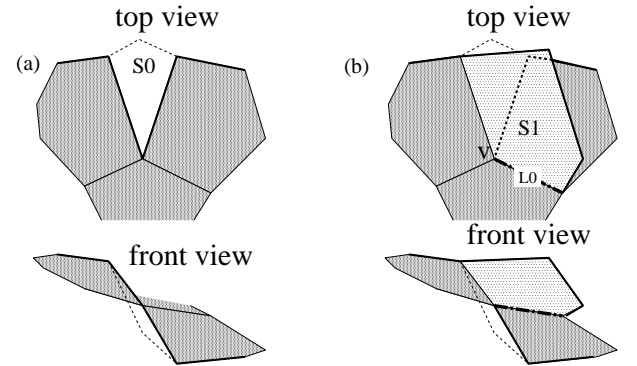


FIG. 6: Schematic depiction of the typical crack branching process observed in the simulation: (a) just before the branching, (b) just after the branching. See the main text for details.

So far, we have shown that in intergranular crack propagation, branching frequently occurs owing to the partial arresting of crack front. Here we infer that this branching behavior may also occur in more general cases of crack propagation in a disordered continuous medium, under some modest assumptions. First, we assume that the crack propagation velocity v mainly and strongly depends on K_I , that is,

$$\frac{\partial v}{\partial K_I} \gg \frac{\partial v}{\partial K_{II}}, \quad \frac{\partial v}{\partial K_I} \gg \frac{\partial v}{\partial K_{III}}, \quad \frac{\partial v}{\partial K_I} \gg \frac{v}{K_I}.$$

For example, a power-law function $v = [K_I^2 + \epsilon(K_{II}^2 + K_{III}^2) - K_c^2]^{a/2}$ satisfies these conditions when $\epsilon \ll 1$ and $a \gg 1$. Secondly, local mode-II stress is assumed to change the crack propagation direction out of the current crack plane so that the mode-I stress normal to the plane increases.

Now consider a straight crack front propagating in an inhomogeneous continuous medium. When the front crosses a small region where mode-II stress is locally induced by inhomogeneous elastic properties, a hump along the vertical direction is generated (Fig. 7). This hump will be eventually lowered owing to the interactions between crack front segments, if the propagating velocity of

each crack front segment does not vary strongly. But the sloped segment feels smaller mode-I stress (by a factor of $\cos \theta$, where θ is an inclination angle of the segment) and its propagating velocity becomes much smaller, say, by a factor of $\cos^a \theta$. This effect may be compensated to some degree, because mode-I stress concentrates on a segment lagged behind. If this compensation is not sufficient, branching of the crack front can occur through a mechanism described below and shown in Fig. 8: (a) The sloped section is lagged behind, owing to the weak mode-I stress at the crack front (b) The left and the right side of the segment bulge inward. (c) The bulged segments further proceed and eventually overlap each other. Then one part shields the stress and continues to proceed, while the other slows down. (d) Owing to mode-II stress induced by the interaction between the crack front segments of overlapped parts, each part gets closer and eventually intersects. (e) Here a segment of the triple junction, or a root of a branch, is formed. (f) A branched “tongue” is left behind and the crack front (now intact) proceeds further. In this way, many small branches are left behind the sweeping crack front also in continuum case.

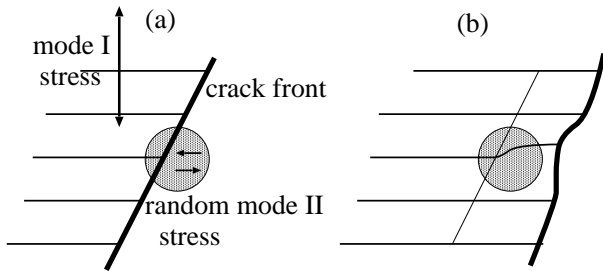


FIG. 7: Schematic picture of humping of crack front propagating in an inhomogeneous medium

In summary, we have modeled and simulated slow intergranular crack propagation, and found that branching of a crack frequently occurs even if explicit branching at grain boundary triple junctions is forbidden. In real intergranular fracture, random crystallographic anisotropy of the elasticity of each grain produces inhomogeneous stress distribution [12] and will enhance crack arresting that leads to more frequent branching. In addition, in the case of polycrystalline metals, a certain portion of GBs are small-angle grain boundaries that are very resistant to fracture and corrosion. Thus, there are numerous arresting GBs and the branching may be strongly enhanced, as observed in IGSCC. We have also inferred that the crack branching mechanism observed in the sim-

ulation of the discrete model may occur in more general cases of crack propagation in a disordered continuous medium, under some modest assumptions on the relation between crack propagation velocity and stress intensity factors. A direct numerical simulation of this continuum case is expected.

The authors would like to thank Masayuki Kamaya, Takashi Tsukada, and Yoshiyuki Kaji for helpful remarks.

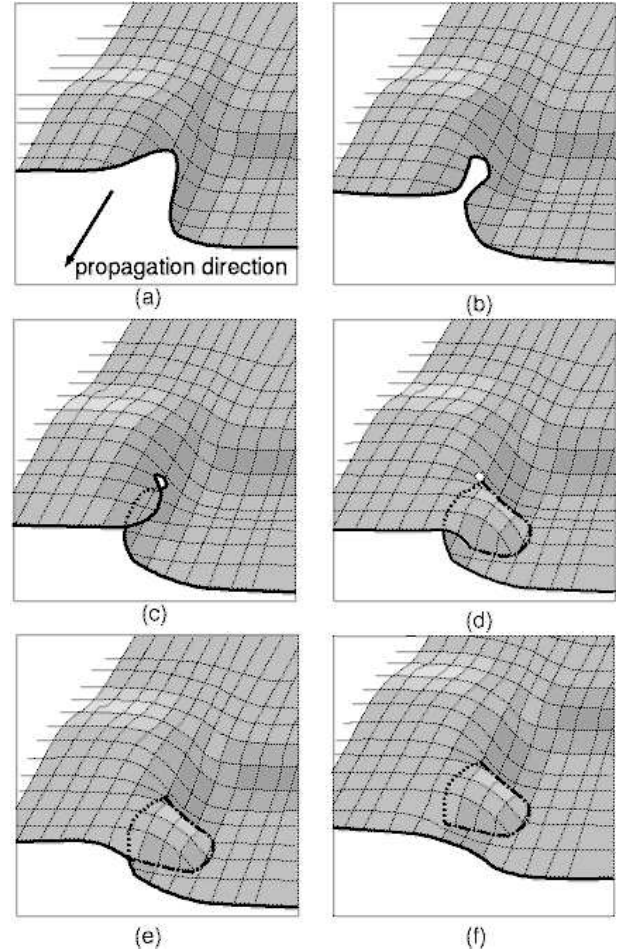


FIG. 8: Schematic picture of the crack branching process expected in a disordered continuous medium. Bold solid lines and bold dotted lines are the crack tip and crack tip under the fracture surface, respectively. The dashed line denotes the triple junction of fracture surface. See the main text for details.

-
- [1] B. B. Mandelbrot, D. E. Passoja, and A. J. Paullay, *Nature* **308**, 721 (1984).
 - [2] F. Célerié, S. Prades, D. Bonamy, L. Ferrero, E. Bouchaud, C. Guillot, and C. Marlière, *Phys. Rev. Lett.* **90**, 075504 (2003).

- [3] E. Sharon and J. Fineberg, *Nature* **397**, 333 (1999).
- [4] A. Karma and A. E. Lobkovsky, *Phys. Rev. Lett.* **92**, 245510 (2004).
- [5] A. Parisi and R. C. Ball, e-print, cond-mat/0403638.
- [6] Y. Tanaka, K. Fukao, Y. Miyamoto, and K. Sekimoto,

- Eurohyps. Lett. **43**, 664 (1998).
- [7] D. Stoyan, W. S. Kendall, and J. Mecke, *Stochastic Geometry and its Applications* (Wiley, Chichester, 1995).
- [8] G. G. Batrouni and A. Hansen, Phys. Rev. Lett. **80**, 325 (1998).
- [9] M. Sahimi and S. Arbabi, Phys. Rev. Lett. **77**, 3689 (1996).
- [10] L. D. Landau and E. M. Lifshitz, *Theory of Elasticity*, (Butterworth-Heinemanni, London, 1995).
- [11] D. G. Harlow, H. M. Lu, J. A. Hittinger, T. J. Delph and R. P. Wei, Modelling Simul. Mater. Sci. Eng. **4**, 261 (1996).
- [12] M. S. Wu and J. Guo, J. App. Mech. **67**, 50 (2000).